

1 **HIV-1 subtype C with PYxE insertion has enhanced binding of Gag-p6 to host**  
2 **cell protein ALIX and increased replication fitness**

3  
4  
5 Robert van Domselaar<sup>1#</sup>, Duncan T. Njenda<sup>2,3#</sup>, Rohit Rao<sup>4</sup>, Anders Sönnnerborg<sup>1,2,4,5</sup>, Kamalendra  
6 Singh<sup>2,4</sup>, Ujjwal Neogi<sup>2\*</sup>

7  
8 <sup>1</sup>Division of Infectious Diseases and Dermatology, Department of Medicine Huddinge,  
9 Karolinska Institutet, Stockholm, Sweden

10 <sup>2</sup>Division of Clinical Microbiology, Department of Laboratory Medicine, Karolinska Institutet,  
11 Stockholm, Sweden

12 <sup>3</sup>Division of Medical Virology, Department of Pathology, Faculty of Medicine and Health  
13 Sciences, Stellenbosch University, Cape Town, South Africa

14 <sup>4</sup>Molecular Microbiology and Immunology, University of Missouri, Columbia, MO 65211, USA

15 <sup>5</sup>Department of Clinical Microbiology and Infectious Diseases, Karolinska University  
16 Laboratory, Karolinska University Hospital, Stockholm, Sweden

17  
18  
19 <sup>#</sup>These authors contributed equally

20  
21  
22 **\*Correspondence:** Ujjwal Neogi, Division of Clinical Microbiology, Department of Laboratory  
23 Medicine, Karolinska Institutet, Stockholm, Sweden, e-mail- [ujjwal.neogi@ki.se](mailto:ujjwal.neogi@ki.se), Phone: +46  
24 852483680

25

26

27 **Abstract**

28 Human immunodeficiency virus type 1 subtype C (HIV-1C) has a natural deletion of a YPxL  
29 motif in its Gag-p6 late domain. This domain mediates the binding of Gag to host cell protein  
30 ALIX and subsequently facilitates viral budding. In a subset of HIV-1C infected individuals, the  
31 tetrapeptide insertion PYxE has been identified at the deleted YPxL motif site. Here, we report  
32 the consequences of PYxE insertion on the interaction with ALIX and the relevance regarding  
33 replication fitness and drug sensitivity. In our three HIV-1C cohorts, PYKE and PYQE were  
34 most prevalent among PYxE variants. Through *in silico* predictions and *in vitro* experiments, we  
35 showed that HIV-1C Gag has an increased binding to ALIX when PYxE motif is present. To go  
36 more into the clinical relevance of the PYxE insertion, we obtained patient-derived gag-pol  
37 sequences from HIV-1C<sub>PYxEi</sub> viruses and inserted them in a reference HIV-1. Viral growth was  
38 increased, and the sensitivity to protease inhibitor (PI) lopinavir (LPV) and nucleoside reverse  
39 transcriptase inhibitor tenofovir alafenamide (TAF) was decreased for some of the HIV-1C PYxE  
40 variants compared to wild-type variants. Our data suggest that PYxE insertion in Gag restores the  
41 ability of Gag to bind ALIX and correlates with enhanced viral fitness in the absence or presence  
42 of LPV and TAF. The high prevalence and increased replication fitness of the HIV-1C virus with  
43 PYxE insertion could indicate the clinical importance of these viral variants.

44 **Importance**

45 Genomic differences within HIV-1 subtypes is associated with a varying degree of viral spread,  
46 disease progression, and clinical outcome. Viral budding is essential in the HIV-1 life cycle and  
47 mainly mediated through the interaction of Gag with host proteins. Two motifs within Gag-p6  
48 mediate binding of host cell proteins and facilitate budding. HIV-1 subtype C (HIV-1C) has a  
49 natural deletion of one of these two motifs resulting in an inability to bind to host cell protein  
50 ALIX. Previously, we have identified a tetrapeptide (PYxE) insertion at this deleted motif site in  
51 a subset of HIV-1C patients. Here, we report the incidence of PYxE insertions in three different  
52 HIV-1C cohorts, and the insertion restores the binding of Gag to ALIX. It also increases viral  
53 growth even in the presence of antiretroviral drugs lopinavir and tenofovir alafenamide. Hence,  
54 PYxE insertion in HIV-1C might be biologically relevant for viruses and clinically significant  
55 among patients.

56

57

58 **Introduction**

59 Human immunodeficiency virus type 1 (HIV-1) is a global threat with an estimated 36.9 million  
60 HIV-1 infected individuals and 940,000 deaths in 2017. Virulence of HIV-1 is determined by its  
61 capacity to replicate within infected cells and its ability to infect new cells. Among different  
62 HIV-1 subtypes, more than 50% of all infections are caused by HIV-1 subtype C (HIV-1C) that is  
63 prevalent in South Africa, Zimbabwe, Mozambique, Botswana, Ethiopia, Eritrea, India, and in  
64 some parts of Brazil. However, HIV-1C has also become highly prevalent in several European  
65 countries, including Sweden (1, 2). The *gag* gene encodes for a polyprotein that is proteolytically  
66 processed by viral and cellular proteases into six final products: p17 matrix protein (MA), p24  
67 capsid protein (CA), spacer peptide 1 (SP1), p7 nucleocapsid protein (NC), spacer peptide 2  
68 (SP2), p6 protein (P6). These proteins are required for the assembly and release of new virions  
69 (3-6). The p6 late domain of Gag contains two conserved short peptide motifs that bind host  
70 factors to facilitate viral budding (6-8). The PTAP motif is present in both HIV-1 and HIV-2, and  
71 sometimes it is duplicated in HIV-1 genomes (9, 10). It mediates binding to ESCRT-I subunit  
72 tumor susceptibility gene 101 (TSG101) (11). The YP<sub>x<sub>n</sub></sub>L (where x<sub>n</sub> represents a random number  
73 of any possible amino acids) motif binds to ESCRT-III adaptor protein ALG-2-interacting protein  
74 X (ALIX) (12). However, this latter motif is deleted exclusively in HIV-1C (13). This deletion is  
75 associated with the loss of binding of p6 late domain to ALIX and a decrease in virus release  
76 from infected cells. Of note, HIV-2 lacks the YP<sub>x<sub>n</sub></sub>L motif but contains an alternative ALIX-  
77 binding motif, namely PYKEVTEDL, that originates from simian immunodeficiency virus (SIV)  
78 in rhesus macaques (14).

79 Recently, we identified a tetrapeptide insertion PYx<sub>n</sub>E [where x represents lysine (K), glutamine  
80 (Q) or arginine (R)] within the Gag protein in a subgroup of HIV-1C infected individuals (C<sub>PYx<sub>n</sub>Ei</sub>-  
81 strains) (15). This C<sub>PYx<sub>n</sub>Ei</sub>-strain was preferentially identified in East African HIV-1C infected  
82 patients but was less common among HIV-1C infected patients from South Africa, India, and  
83 Germany (15). Furthermore, the insertion appears more frequent among patients on antiretroviral  
84 therapy, e.g., ritonavir-boosted protease inhibitors (PI), compared to therapy naïve patients in  
85 India, and more frequent in therapy-failure patients in South Africa (15, 16). Moreover, lower  
86 pre-therapy CD4<sup>+</sup> T cell counts, higher plasma viral loads, and reduced increase in CD4<sup>+</sup> T cell

87 counts were noted to be associated with PYxE insertion in HIV-1C patients compared to patients  
88 with wild type HIV-1C from East Africa (17). Furthermore, we observed that increased  
89 replication fitness in PYQE inserted HIV-1C viruses was polymerase independent (17). A more  
90 recent study also claimed that gag-protease is the major determinant of subtype differences in  
91 disease progression among HIV-1 subtypes (18).

92 As the tetrapeptide PYxE insertion was found at the site of the lost YPx<sub>n</sub>L motif of HIV-1C Gag-  
93 p6, we hypothesized that this PYxE insertion might restore the interaction of the Gag-p6 late  
94 domain with ALIX and thereby increases replication fitness and reduces sensitivity to PIs. A  
95 recent report showed that the PYRE insertion could rescue the viral growth of a PTAP-deleted  
96 HIV-1 variant similar to the YPx<sub>n</sub>L motif in the absence of a PTAP sequence (19). However,  
97 since the PTAP motif is always present in clinical HIV-1 isolates, it is not known if and how  
98 PYxE insertion affects HIV-1C pathogenicity in a clinically relevant context. To address this, we  
99 assessed the distribution and frequency of this PYxE insertion in different cohorts of HIV-1C  
100 infected individuals. We also evaluated the ability of PYxE motif to reconstitute the interaction of  
101 Gag with ALIX, its association with increased viral growth of clinical isolates, and its association  
102 with drug responses against all three drug classes; reverse transcriptase inhibitors (RTIs), PIs, and  
103 integrase strand transfer inhibitors (INSTIs).

## 104 **Material and Methods**

### 105 *Cell culture and plasmids*

106 Cells were cultured in 5% CO<sub>2</sub> at 37°C. HEK293T cells were maintained in Dulbecco's modified  
107 Eagle medium (DMEM, Sigma, USA) supplemented with 10% fetal calf serum (Sigma, USA), 2  
108 mM L-glutamine (Sigma, USA), 0.1 mM MEM Non-Essential Amino Acids (Gibco/Thermo  
109 Fisher Scientific, USA), and 10 units/mL penicillin combined with 10 µg/mL streptomycin  
110 (Sigma). TZM-bl reporter cells were also maintained in medium mentioned above. This reporter  
111 cell line is a derivative of HeLa cells, but stably expresses high levels of CD4 and CCR5 on the  
112 cell surface, and has integrated copies of the luciferase gene under the control of the HIV-1  
113 promoter that allows simple and quantitative analysis of HIV-1 infection. MT-4 cells were  
114 maintained in Roswell Park Memorial Institute 1640 (RPMI, Sigma, USA) medium  
115 supplemented with 10% fetal calf serum, 20 units/mL penicillin and 20 µg/mL streptomycin.

116 Cells were transfected using FuGene HD according to the manufacturer's instructions (Promega,  
117 USA) in a 3:1 ratio with DNA.

118 The pEGFPN1 and mCherry plasmids were obtained from Addgene (Addgene, USA). The  
119 plasmid encoding for HA-tagged ubiquitin was a kind gift from Soham Gupta (Karolinska  
120 Institutet, Sweden). pCR3.1/HIV-Gag-mCherry (HIV-1B Gag ) and pCR3.1-GFP-ALIX plasmids  
121 were kind gifts from Dr. Paul Bieniasz (The Rockefeller University, USA). A codon-optimized  
122 HIV-1 Gag with PYQE motif gene of East African HIV-1C viruses was cloned into the  
123 pCR3.1/HIV-Gag-mCherry plasmid that contained an mCherry protein C-terminal tag sequence.  
124 The Gag-PYQE-mCherry plasmid was modified by site-directed mutagenesis to make a base pair  
125 substitution mutation (C to A) that changes the PYQE motif to PYKE using the Q5 SDM kit  
126 (New England Biolabs, USA). Gag-PYQE-mCherry plasmid was linearized by PCR using 5'-  
127 AAGGAGCCTCTGACGAGCC-3' as forward primer (with the C to A base pair substitution  
128 underlined) and 5'-ATAGGGACCCTGGTCTTTCAGC-3' as reverse primer. Linear products  
129 were re-circularized using DpnI, a polynucleotide kinase and a ligase from the SDM kit following  
130 the manufacturer's protocol. DNA sequences were verified by Sanger sequencing.

### 131 *Gag-p6 sequences and clinical specimens*

132 To identify the distribution of PYQE, PYRE and PYKE motifs, we re-analysed the HIV-1C gag-  
133 p6 sequences that were collected from three cohorts, the Swedish InfCare Cohort (n=140), the  
134 German Cohort (n=127), and the Ethiopian Cohort (n=73), as reported previously with respect to  
135 naturally occurring polymorphisms in PYx<sub>E</sub> motif (15). Additional HIV-1B (n=2754) and HIV-  
136 1C (n=1432) gag-p6 sequences were collected from HIV-1 Los Alamos Database. Stored plasma  
137 samples from therapy naïve patients infected with HIV-1C (n=10) were randomly selected based  
138 on gag-p6 sequences from the HIV-cohort at Karolinska University Hospital, Stockholm,  
139 Sweden.

### 140 *Recombinant virus production with patient-derived gag-pol*

141 The recombinant viruses were produced as described by us recently (20). Briefly, the *gag-pol*  
142 fragment (HXB2:0702-5798) was cloned into pNL4-3 plasmid following digestion with *Bss*HII  
143 and *Sall* (New England Biolab, USA) and ligation using T4 DNA ligase (New England Biolabs,  
144 USA). The chimeric viruses were produced by transient transfection of the plasmids into the

145 293T cell line using FuGene HD and harvested 72 hours later by a collection of the cell-free  
146 supernatant cleared by centrifugation and stored in aliquots at -80°C.

147 *In silico analysis: Molecular modeling, docking, and Ubiquitin binding motif prediction*

148 Homology modeling techniques generated the structure of HIV-1C Gag late domain with the  
149 PYKE insertion. The published crystal structures of the Gag late domain in complex with ALIX  
150 (PDB entries 2XS1 (14) and 2R02 (21)) were used as template molecules to model HIV-1C Gag  
151 late domain. For this purpose, the 'Prime' utility of Schrödinger Suite (Schrödinger Inc., USA)  
152 was used. The structure was subjected to restricted minimization using OPLS\_2005 force field.  
153 The resulting structure of HIV-1C Gag late domain structure was docked into the crystal structure  
154 of ALIX (PDB file 2XS1) using PIPER protein-protein docking program of BioLuminate Suite  
155 (Schrödinger Inc., USA), after deleting SIV<sub>mac239</sub> PYKEVTEDL late domain structure. The  
156 resulting structure was further minimized for 1000 iterations to remove steric clashes. A similar  
157 protocol was used to form the complex among ALIX, Gag late domain, and ubiquitin. The crystal  
158 structure of ubiquitin in complex with the TSG101-binding PTAP domain (PDB file 1S1Q) was  
159 used after deleting TSG101 coordinates (22). The entire complex was then subjected to molecular  
160 dynamics simulations for 1,000,000 steps with step size of 50 picoseconds using an OPLS3 force  
161 field. The most energetically stable model of the complex was used for further analysis. To obtain  
162 energetically favored polar interactions, the conformational search of polar sidechains at the  
163 interface of proteins was also conducted.

164 The prediction of ubiquitin binding with the HIV-1C Gag late domain with the PYKE motif P6  
165 was performed by adding the amino acid sequence in the prediction tools presented at the website  
166 <http://www.ubpred.org/>.

167 *Immunofluorescence*

168 HEK293T cells were cultured on poly-L-lysine-coated glass coverslips and co-transfected with  
169 GFP-tagged ALIX and mCherry-tagged codon-optimized Gag variants. At 24 hours post-  
170 transfection, cells were washed twice with PBS, fixed in 10% formalin (Sigma, USA) for 20 min  
171 at room temperature, washed three times with PBS, and stored in PBS at 4°C. Later, nuclear  
172 counterstaining with DAPI was performed followed by mounting of the glass coverslips on glass  
173 slides. When HA-ubiquitin was also co-transfected, cells were fixed in ice-cold methanol for 15  
174 min at -20°C, washed twice with PBS, and stored in PBS at 4°C. For ubiquitin detection, fixed

175 cells were incubated with the anti-HA antibody (mouse monoclonal, clone 12CA5, Sigma, USA)  
176 for 1 hour at room temperature followed by goat-anti-mouse-Alexa Fluor 647-Plus-conjugated  
177 secondary antibody (Invitrogen, USA) for 1 hour at room temperature before nuclear  
178 counterstaining with DAPI. Fluorescence was analyzed by confocal laser scanning microscopy  
179 using a Nikon Single point scanning confocal microscope with  $\times 60/1.4$  oil objective (Nikon,  
180 Japan). Fluorescence intensity was measured (along drawn lines) using Fiji/ImageJ software (23).  
181 The highest fluorescence intensity value for each fluorophore along each line was set to 100%,  
182 and values were plotted as relative fluorescence intensity in percentage against distance in  
183 microns using GraphPad Prism v6 (Graphpad Inc., USA).

#### 184 *Microscale Thermophoresis (MST)*

185 The microscale thermophoresis experiments were conducted by Monolith NT0.115 instrument  
186 (NanoTemper Technologies) at 40% MST and LED power at 25°C. Hexahistidine-tagged ALIX  
187 protein was labeled by NTA-dye (NanoTemper Technologies) using manufacturer's protocol.  
188 The peptides were synthesized at the Molecular Interaction Core (University of Missouri).  
189 Thermophoresis was induced by mixing peptides (0.001-1  $\mu$ M) and fixed NTA-labelled ALIX (50  
190 nM) in a buffer 50 mM Tris-Cl pH 7.8, 100 mM NaCl and 0.1% pluronic-F127. The binding  
191 isotherms were obtained by plotting the difference in normalized fluorescence against increasing  
192 peptide concentration. The binding affinities were determined to fit the data points to a quadratic  
193 equation (equation 1) using non-linear regression using MO Affinity software (NanoTemper  
194 Technologies), Prism (GraphPad Inc. version 6.0) or OriginLab (version 18, OriginLab Corp.  
195 Northampton, MA, USA).

$$196 \quad F_b = \frac{(K_{d1} + [PEP_0] + [ALIX_0]) - \sqrt{(K_{d1} + [PEP_0] + [ALIX_0])^2 - 4[ALIX_0][PEP_0]}}{2[ALIX_0]} \quad (\text{Eq. 1})$$

197 Where  $F_b$  is fraction of ALIX/peptide complex, where  $K_d = [ALIX][PEP]/[ALIX-PEP]$ , [ALIX]  
198 is the concentration of free ALIX,  $[ALIX_0]$  is the concentration of total ALIX, [PEP] is the  
199 concentration of free peptide and  $[PEP_0]$  is the total concentration of peptide.

#### 200 *Co-immunoprecipitation assay*

201 HEK293T cells were co-transfected with GFP-tagged ALIX and codon-optimized Gag variants  
202 from HIV-1B or HIV-1C. At 24 hours post-transfection, cells were collected, washed twice with  
203 ice-cold PBS and immunoprecipitation of GFP-tagged proteins was performed using GFP-

204 Trap®\_A kit (Chromotek, Germany) according to the manufacturer's protocol. Briefly, cells  
205 were lysed in ice-cold lysis buffer (10 mM Tris pH 7.5, 150 mM NaCl, 0.5 mM EDTA, 0.5%  
206 NP-40, supplemented with a protease cocktail inhibitor from Roche, Switzerland) for 30 minutes  
207 on ice. Then lysates were diluted in ice-cold wash buffer (10 mM Tris pH 7.5, 150 mM NaCl, 0.5  
208 mM EDTA) supplemented with a protease cocktail inhibitor from Roche, input samples (10% of  
209 total) were saved for immunoblot analysis, and the remaining (90%) part of the diluted lysates  
210 were incubated with equilibrated GFP-Trap®\_A beads end-over-end for 1 hour at 4°C. Beads  
211 were washed three times with ice-cold wash buffer before resuspending in 2x Leammi buffer  
212 (Invitrogen, 4x buffer diluted 1:1 with PBS) and heated for 10 minutes at 95°C. The protein  
213 concentration of input samples was determined by DC protein assay (Biorad, USA) according to  
214 the manufacturer's microplate assay protocol. Equal amounts of protein for input samples and  
215 equal volumes of pull-down samples were subjected to immunoblotting using primary antibodies  
216 against GFP (rabbit monoclonal, clone EPR14104, Abcam, UK), Gag (rabbit polyclonal to HIV1  
217 p55 + p24 + p17, Abcam, ab63917), and  $\beta$ -actin (rabbit polyclonal, Abcam, ab8227) and  
218 secondary horseradish peroxidase-conjugated antibodies (polyclonal goat anti-rabbit,  
219 DAKO/Agilent, USA). Immunoblotted proteins were detected using the enhanced  
220 chemiluminescence detection system (Pierce/Thermo Fisher Scientific, USA) and Hyperfilms  
221 (Amersham/GE Healthcare Life Sciences, UK).

#### 222 *Viral growth kinetics assay in MT-4 cell*

223 First, TCID<sub>50</sub> for each propagated recombinant viral clone was determined in TZM-bl reporter  
224 cells. For each recombinant viral clone, ten-fold serial dilutions were prepared to range from 10<sup>2</sup>  
225 to 10<sup>7</sup> in dilution factor from a single aliquot in medium containing DEAE (20  $\mu$ g/ $\mu$ L). TZM-bl  
226 cells were plated in 96-well plates, and six replicates were incubated with the various virus  
227 dilutions for 48 hours at 37°C in a 5% CO<sub>2</sub> humidified incubator. Virus infectivity was quantified  
228 by measuring Renilla luciferase activity (relative light units [RLU]) using Bright-Glo™  
229 Luciferase Assay System (Promega, USA) on the Tecan microplate reader (Tecan Infinite® 200  
230 Pro, Tecan Group Ltd, Switzerland). The Spearman-Kärber method was used to calculate the  
231 TCID<sub>50</sub> for each recombinant viral clone. Then, MT-4 cells (2 x 10<sup>5</sup>) were seeded in a 12-well  
232 plate and infected with each recombinant virus at a multiplicity of infection (MOI) of 0.05  
233 plaque-forming units (pfu) per cell in triplicates for each condition. Supernatants were collected  
234 on day 0, 3, 5 and 7 days post infection, and HIV-1 p24 levels in supernatants were measured on



235 the HIV COBAS 8000 platform (Roche Diagnostics, Switzerland). Viral growth kinetics (VGK)  
236 were analyzed as a relationship between signal to the cut-off ratio (i.e., electrochemiluminescence  
237 signal of the sample relative to calibrated negative samples for the HIV combi PT kit on the  
238 COBAS 8000 system) for each time point and replicate. Graphical representation of the result  
239 was made using Graphpad Prism v6 (Graphpad Inc., USA).

#### 240 *Isolation of CD4<sup>+</sup> T-cells*

241 Primary CD4<sup>+</sup> T-cells were isolated from donor peripheral blood mononuclear cells (PBMCs).  
242 Briefly, 4.3 x 10<sup>8</sup> PBMCs were obtained from 50 ml buffy coat using the standard method of  
243 gradient separation using Ficoll Histopaque reagent followed by centrifugation. Isolated PBMCs  
244 were used to isolate CD4<sup>+</sup> T-cells by negative selection using the EasySep<sup>TM</sup> Human CD4<sup>+</sup> T-  
245 cells isolation kit (Stem Cell Technologies, Canada). Briefly, PBMCs were pooled in 5 mL  
246 polystyrene round-bottom tubes at a concentration of 5 x 10<sup>7</sup> cells and incubated with 50 µL of an  
247 antibody cocktail for 5 min at room temperature before mixing with RapidSphere<sup>TM</sup> beads  
248 followed by magnetic separation to yield pure CD4<sup>+</sup> T-cells.

#### 249 *Viral growth kinetics assay in CD4<sup>+</sup> T-cells*

250 CD4<sup>+</sup> T-cells were cultured using RPMI media supplemented with 10% fetal calf serum and 1%  
251 pen-strep (penicillin and streptomycin). The cells were stimulated with PHA (20 µg/ml final  
252 concentration) for three days before starting the assay. To start the viral growth kinetics assay, 1  
253 x 10<sup>6</sup> CD4<sup>+</sup> T-cells were seeded in each well in a V- bottom 96-well culture plate and infected  
254 with viruses at an M.O.I of 0.05 pfu/cell in the presence of 20 µg/mL of DEAE. The plate was  
255 spinoculated at 37°C for 2 hours at 800 rpm in a temperature-controlled centrifuge. After that, the  
256 plate was further incubated in a 5% CO<sub>2</sub> incubator for 8 hours. Afterward, infected cells were  
257 transferred to a 48-well culture plate and washed six times before harvesting the initial  
258 supernatant from each corresponding well and designating it Day 0. The experiment was then  
259 monitored for seven days, and the supernatant was harvested for days 3, 5 and 7. HIV p24 was  
260 then measured in the supernatants using HIV alliance p24 ELISA kit (Pekin Elmer, USA) and  
261 results were analyzed using GraphPad Prism v6 (Graphpad Inc., USA).

#### 262 *Drug sensitivity assay (DSA)*

263 The following drugs were purchased from Selleckchem, USA: Atazanavir sulfate (ATV),  
264 darunavir ethanoate (DRV), lopinavir (LPV), azidothymidine (AZT), tenofovir alafenamide

265 (TAF), efavirenz (EFV), rilpivirine (RPV), etravirine (ETR), raltegravir (RAL), elvitegravir  
266 (EVG), dolutegravir (DTG), and cabotegravir (CAB).. The DSA was performed by determining  
267 the extent to which the antiretroviral drug inhibited the replication of the reference virus (pNL4-  
268 3), wild-type, PTAPP duplicated, and PYxE derived recombinant viruses, respectively. One  
269 round was required for all drugs as previously reported (20), except for the protease inhibitor (PI)  
270 drugs that required two rounds of infection. Briefly for the for two-round infection using PI DSA,  
271 TZM-bl cells ( $1 \times 10^4$ ) were seeded in 96-well plates and cultured for 24 hours. Drugs were  
272 serially diluted in culture media (ranging from 0.1  $\mu$ M to 0.01 pM) and added in triplicate to the  
273 cells. The following day, viruses were added to each well at an MOI of 0.05 pfu/cell in the  
274 presence of DEAE (10  $\mu$ g/ml). After 48 hours, the viral supernatant from respective 96-wells  
275 plates with each drug was transferred to newly TZM-bl pre-seeded 96-wells plates without  
276 adding new drugs. After that, virus replication was quantified by measuring Renilla luciferase  
277 activity (relative light units [RLU]) using Bright-Glo™ Luciferase Assay System (Promega,  
278 USA) 48 hours post-reinfection. Drug concentrations required for inhibiting virus replication by  
279 50% ( $EC_{50}$ ) were calculated by a dose-response curve using non-linear regression analysis  
280 (GraphPad Prism, version 6.07; GraphPad Software, USA). The DSA experiments were  
281 performed with three technical replicates for each virus with the specified dynamic concentration  
282 range of the drug, and at least two independent analyses were performed. The reproducibility of  
283 the DSA was assessed by the 95% confidence interval obtained for the drug  $EC_{50}$  and the degree  
284 of correlation between technical replicates. The output for the drug  $EC_{50}$  results was used to  
285 compute the fold change value (FCV) for each virus relatively to pNL4-3.

286

287

288 **Results**289 *Evolution of gag-p6 late domain sequences in HIV-1B and HIV-1C*

290 The sequence analysis of HIV-1B and South African and Indian HIV-1C gag-p6 sequences  
291 (obtained from the Los Alamos Database) identified a conserved LYP<sub>x</sub>nL motif in HIV-1B which  
292 was missing in HIV-1C (Fig 1a). We noted a unique evolution of the lysine (K) residue in the  
293 HIV-1B and HIV-1C gag-p6 late domain, which is the target of ubiquitination. All the amino  
294 acids positions are per the standard HXB2 co-ordinates. While K475 residue was conserved in  
295 both HIV-1B and C, there was an evolution of a lysine residue at amino acid position 479 along  
296 with K481R mutation in the majority of HIV-1C sequences. Interestingly, the multiple sequence  
297 alignment of HIV-1C<sub>PYx<sub>E</sub>Ei</sub> strains identified conservation of HIV-1C specific K479 residue, but  
298 residue R481 in HIV-1C<sub>WT</sub> changed to a lysine residue within HIV-1C<sub>PYx<sub>E</sub>Ei</sub> strains and thus  
299 identical to K481 in HIV-1B (Fig 1a). When we analyzed gag-p6 sequences from HIV-1C  
300 patients from the Swedish InfCare HIV cohort (n=140), we found that 68% (95/140) of HIV-1C  
301 patients had a wild type strain whereas 32% (45/140) had a PYx<sub>E</sub> insertion; 22% (31/140) had a  
302 PYKE insertion, and 9% (13/140) had a PYQE insertion (Fig.1b). All of the PYx<sub>E</sub> sequences in  
303 HIV-1C of patients from the Swedish cohort belonged to HIV-1C strains of Ethiopian and  
304 Eritrean origin. A similar trend was observed in the German HIV-1C cohort with 12% PYKE  
305 insertion (15/127) (Fig.1c), and in the Ethiopian HIV-1C cohort with 37% (27/73) PYKE  
306 insertion (Fig. 1d). Thus, our analysis indicated that PYKE and PYQE are predominating in HIV-  
307 1C<sub>PYx<sub>E</sub>Ei</sub> viruses of all cohorts analyzed. Subsequently, we restricted our analysis to these two  
308 variants.

309 *PYx<sub>E</sub> insertion enhances type C Gag: ALIX interaction*

310 Before testing the interaction between Gag and ALIX, we evaluated the cellular localization of  
311 both proteins. 293T cells were co-transfected with GFP-tagged ALIX with or without three  
312 codon-optimized variants of mCherry-tagged HIV-1C Gag, namely wild type Gag or Gag that  
313 includes the tetrapeptide insertion PYKE or PYQE. Confocal analysis showed cytoplasmic  
314 localization of ALIX and predominant plasma membrane localization of all three Gag variants  
315 (HIV-1C<sub>WT</sub>, HIV-1C<sub>PYQE<sub>Ei</sub></sub>, and HIV-1C<sub>PYKE<sub>Ei</sub></sub>) as the complete Gag produces virus-like particles  
316 (Fig.2). Thus, the tetrapeptide insertion did not cause a change or defect in the localization  
317 pattern of Gag proteins at the plasma membrane.

318 Next, we evaluated the binding affinity of four HIV-1 Gag variants, HIV-1B<sub>WT</sub>, HIV-1C<sub>WT</sub>, HIV-  
319 1C<sub>PYKEi</sub>, and HIV-1C<sub>PYQEi</sub>, to ALIX (Fig 3a). The late domain motifs' peptides were selected  
320 based on crystal structure PDB:2XS1 and PDB:2R02. The binding affinity of the Gag peptide  
321 with ALIX was statistically significantly higher in HIV-1B<sub>WT</sub> ( $32 \pm 3$  nM) compared to all HIV-  
322 1C variants; HIV-1C<sub>WT</sub> ( $290 \pm 6$  nM), HIV-1C<sub>PYKEi</sub> ( $110 \pm 4$  nM), HIV-1C<sub>PYQEi</sub> ( $96 \pm 4$  nM) (Fig  
323 3b). However statistically significant higher binding affinity to ALIX was observed with HIV-  
324 1C<sub>PYKEi</sub> and HIV-1C<sub>PYQEi</sub> compared to HIV-1C<sub>WT</sub>.

325 As the peptides may not retain their conformational structures as in the complete protein, we  
326 confirmed the binding by co-immunoprecipitation pull-down assays. GFP-tagged ALIX and  
327 HIV-1C Gag variants were transfected either alone or together in 293T cells. A plasmid encoding  
328 for HIV-1B Gag was used together with GFP-ALIX as a positive control for Gag:ALIX  
329 interaction. Lysates were prepared 24 hours post-transfection, GFP-tagged proteins were pulled  
330 down, and co-immunoprecipitated proteins were analysed by immunoblotting (Fig.3c). Pull down  
331 of GFP-tagged ALIX was efficiently and the amount of HIV-1B Gag was increased when it was  
332 co-transfected with GFP-ALIX confirming that HIV-1B Gag binds to ALIX. HIV-1C Gag wild  
333 type was also detected when co-transfected with GFP-ALIX, but HIV-1C Gag PYKE was more  
334 prominently detected. The intensity of HIV-1C Gag PYQE was consistently lower than that of  
335 the PYKE variant but slightly increased compared to the wild type HIV-1C Gag. Thus, the  
336 tetrapeptide insertion PYxE in HIV-1C Gag-p6 late domain promotes binding of Gag towards  
337 ALIX.

### 338 *In silico analysis predicts binding of ALIX to the PYKE motif in Gag facilitated by ubiquitination*

339 As reported before, the lysine residues in the Gag-p6 are subjected to ubiquitination (24), we first  
340 predicted the likelihood of ubiquitination of the lysine residue of PYKE ( $K_{ins}$ ) compared to lysine  
341 residues adjacent to the PYKE motif. Indeed,  $K_{ins}$  was predicted to be more likely ubiquitinated  
342 than lysine residues in the vicinity of the PYKE motif (Fig.4a). Since the PYKE motif is present  
343 at the missing ALIX-binding site and contains three charged amino acids that can facilitate  
344 interaction with other proteins, we used the PYKE insertion (amino acids 483 to 486) in the  
345 molecular modeling to predict the interaction of the Gag-p6 late domain with ALIX. Amino acids  
346 E482, Y484 and E486 of Gag could directly facilitate binding to ALIX (Fig.4b and Table 1).  
347 Ubiquitin was predicted to bind K501 in ALIX and thereby affected the interaction between E486

348 in Gag-PYKE with K501 in ALIX. Besides, ubiquitin could also interact with E387 of ALIX and  
349  $K_{ins}$  of Gag-PYKE through its residues K63 and E64, respectively. Thus, our *in silico* analysis  
350 predicted that the PYx<sub>E</sub> motif could restore the interaction of Gag with host cell ESCRT-III  
351 adaptor protein ALIX and that, in case of a PYKE insertion, ubiquitination of the  $K_{ins}$  residue  
352 could further facilitate this interaction. We also tested the localization of ubiquitin by  
353 immunofluorescence. Since both Gag and ALIX are known to be ubiquitinated, it was not  
354 surprising that ubiquitin co-localized with ALIX and Gag (Fig.4c).

#### 355 *Differences in viral growth of clinical strains of HIV-1C with PYx<sub>E</sub> motif*

356 Finally, we assessed the consequence of the PYx<sub>E</sub> insertion on HIV-1C replication fitness using  
357 clinical strains obtained from HIV-1C infected patients. Gag-pol sequences were cloned from one  
358 wild type HIV-1C virus with a single PTAP motif and no PYx<sub>E</sub> insertion (PT01), three HIV-1C  
359 strains with a PYKE insertion (PT04-06), and one with a PYQE insertion (PT07). We also  
360 included two HIV-1C strains with a PTAP duplication (PT02 and PT03) as it has been shown to  
361 increase the viral fitness and affect the drug sensitivity (Fig.5a) (25, 26). Then, these sequences  
362 were cloned into the genome of a reference virus (NL4-3, HIV-1B wild type) replacing its gag-  
363 pol sequence. The various recombinant viruses were tested for viral replication in an *ex vivo* viral  
364 growth kinetic assay and compared to the reference virus in MT-4 cell line (Fig.5b) and primary  
365 CD4<sup>+</sup> T-cells isolated from donor blood (Fig 5c). In MT-4 cells, a statistically lower amount of  
366 HIV-1C<sub>WT</sub> virus was observed in the supernatant compared to the HIV-1C<sub>PYx<sub>E</sub></sub> and HIV-1B  
367 reference viruses 3 days post infection. At day 5 post infection, the amount of HIV-1C<sub>WT</sub> virus  
368 was still reduced compared to the other viruses. The amount of HIV-1C<sub>WT</sub> in the supernatant was  
369 highest at day 7 post-infection. The reduction of HIV-1C<sub>PYx<sub>E</sub></sub> and HIV-1B viruses at day 7 post-  
370 infection is most likely caused by the death of the virus-producing cells, which was observed  
371 microscopically. Similar data was observed in CD4<sup>+</sup> T-cells where HIV-1C<sub>WT</sub>, compared to all  
372 other viruses, showed the lowest amount of virus in the supernatant 7 days post-infection (Fig.  
373 5c). Our data that viral replication for the HIV-1C wild type clone was reduced compared to the  
374 HIV-1B reference virus is in concordance with a previous report (27). More importantly, our data  
375 showed that when a PTAP-duplication or a PYx<sub>E</sub> insertion was present, viral growth was  
376 increased compared to the HIV-1C wild type variant and was comparable to HIV-1B wild type.  
377 This correlation suggests that HIV-1C strains with a PYx<sub>E</sub> insertion have a growth advantage

378 compared to wild type HIV-1C. This is also in line with our earlier study that HIV-1C<sub>PYQEi</sub>  
379 viruses are more replication competent as well as more pathogenic (17).

380 Next, we checked whether the *ex vivo* data corroborate with the clinical data. In the Swedish  
381 HIV-1C cohort (n=140) we checked the nadir CD4<sup>+</sup> T-cell count, CD4<sup>+</sup> T-cell count at the  
382 initiation of therapy, and viral load at initiation of therapy. The viral load was significantly higher  
383 in HIV-1C<sub>PYxEi</sub> infected individuals compared to the individuals who were infected with wild  
384 type HIV-1C viruses (Fig 5d). The CD4<sup>+</sup> T-cell count at the initiation of therapy (Fig 5e) and  
385 nadir CD4<sup>+</sup> T-cell count (Fig 5f) were also statistically lower in the HIV-1C<sub>PYxEi</sub> infected  
386 individuals compared to individuals infected with wild type HIV-1C viruses. These data further  
387 strengthen our *ex vivo* findings.

#### 388 *Effect of PYxE strains in susceptibility towards antiretroviral drugs*

389 Several reports have shown that a PYxE insertion is more frequent among HIV-1C therapy  
390 failure patients (16, 28). To examine whether recombinant viral clones without any known drug  
391 resistance mutations to RTIs, PIs and INSTIs responded differently to various antivirals, the  
392 target cells were infected with individual viral clones in the presence of a specific drug. The viral  
393 replication was assessed, and the EC<sub>50</sub> was calculated and fold change of the EC<sub>50</sub> was mentioned  
394 (Fig. 6). No differences in EC<sub>50</sub> values were observed among the various recombinant viral  
395 clones in the presence of non-nucleoside RTIs (NNRTIs) efavirenz (EFV), rilpivirine (RPV) or  
396 etravirine (ETR), or INSTIs raltegravir (RAL), elvitegravir (EVG), dolutegravir (DTG) or  
397 cabotegravir (CAB).

398 In contrast, with the PI lopinavir (LPV) one out of two viral clones with a PTAP-duplication and  
399 two out of four with PYxE insertion showed a >4-fold decreased sensitivity towards the drug.  
400 However, there was no change in susceptibility against DRV and ATV. One of the other viral  
401 clones with a PYxE insertion showed a 3.5-fold decreased sensitivity towards nucleoside reverse  
402 transcriptase inhibitor (NRTI) tenofovir alafenamide (TAF). Thus, our data indicate that PYxE  
403 insertion may potentially alter the sensitivity towards the PI LPV and NRTI TAF and that may be  
404 due to the increased replication fitness. However, this is not universal across all the HIV-1<sub>PYxEi</sub>-  
405 strains and could be due to co-evolution of other amino acids in the Gag protein.

406

407 **Discussion**

408 Genetic diversity among HIV-1 strains and their adaptation can provide advantages for individual  
409 viral strains in different biological contexts. Here, we described the distribution of HIV-1C  
410 containing tetrapeptide PYxE insertion within Gag and assessed the binding efficiency of Gag  
411 with host cell protein ALIX. Our results showed that the PYxE insertion enhances the binding  
412 capacity of HIV-1C Gag to ALIX in a potentially ubiquitin-dependent or independent manner.  
413 Also, the insertion increased the replication fitness of the virus in both an *in vitro* model using a T  
414 cell line as well as in primary CD4<sup>+</sup> T cells and seemed to alter the sensitivity against the PI LPV  
415 and NRTI TAF in some of the strains.

416 Although the PYxE insertion is quite prevalent among HIV-1C from Ethiopia and Eritrea  
417 individuals, it is not as prevalent in South African or Indian HIV-1C strains (16, 28). The twelve  
418 base pair sequence encoding the PYxE motif is not present in non-subtype C M group HIV-1  
419 sequences but is present within the Gag-p6 late domains of SIV<sub>mac239</sub>, SIV<sub>smE543</sub>, and their close  
420 relative HIV-2 (14, 29). As HIV-1C has a natural deletion of the YP<sub>x<sub>n</sub></sub>L motif and insertion of  
421 PYxE has replication advantages, we hypothesize that these strains have evolved through a  
422 recombination event of HIV-1C with either SIV or HIV-2. It is well described that the HIV-1  
423 epidemic in Ethiopia geographically clusters very strongly (30) and the Ethiopian HIV-1C has  
424 been proposed to originate from either a single lineage or multiple descendants (31). However to  
425 explain why the PYxE insertion is significantly more prevalent in HIV-1C from Ethiopia and  
426 Eritrea as compared to South African and Indian strains needs a further evolutionary study to  
427 prove this hypothesis.

428 The Gag-p6 late domain mediates viral budding through the PTAP motif, the YP<sub>x<sub>n</sub></sub>L motif, and  
429 the PYxE motif. The PTAP motif mediates binding of Gag to ESCRT protein TSG101 and is  
430 present in all HIV and SIV variants. Therefore, this domain appears to be necessary for viral  
431 budding. Although one report shows that PTAP duplication only increases HIV-1 replication in  
432 the presence of a PI (26), others and we observed increased viral growth when HIV-1 contained a  
433 PTAP duplication (25). Although deletion of the PTAP motif has not been identified in clinical  
434 strains so far, artificial deletion or mutation of this PTAP motif severely abrogates release of  
435 HIV-1 from infected cells (11, 32, 33). However, the presence of either one of the two other  
436 motifs that both facilitate binding to host cell protein ALIX still allows for virion release (12, 14,

437 19, 34, 35). This indicates that both TSG101- and ALIX-mediated pathways for viral budding are  
438 not dependent on each other and each pathway is sufficient to mediate viral budding. The first  
439 ALIX-binding motif is YP<sub>x</sub><sub>n</sub>L and is present in most HIV-1 subtypes but not in HIV-1C or HIV-  
440 2 (13, 14). HIV-2 Gag can mediate binding to ALIX through a distinct PYKEVTEDL motif, and  
441 mutations in this motif can abrogate ALIX binding and decrease virion release (14, 29). Thus, the  
442 PY<sub>x</sub>E motif in a subgroup of HIV-1C strains is similar but shorter than the ALIX-binding motif  
443 found in HIV-2. We showed that this insertion of PY<sub>x</sub>E in HIV-1C Gag at the natural deletion  
444 site of the YP<sub>x</sub><sub>n</sub>L domain could reconstitute binding of HIV-1C Gag to ALIX. Hence, together  
445 with our observed PY<sub>x</sub>E insertion in HIV-1C, all HIV-1 subtypes have an ALIX-binding motif  
446 next to their PTAP-motif within the Gag late domain.

447 Our data suggest that ubiquitin may play a role in facilitating the binding of ALIX to the PYKE  
448 motif. This is not surprising, as ubiquitin has been shown to be involved in viral budding of HIV.  
449 Although dispensable for virus budding, ubiquitination of Gag and the ESCRT-proteins are  
450 essential for efficient release of HIV-1 from infected cells (24, 36, 37). Ubiquitination of the  
451 lysine of the PYKE motif could increase the binding between ALIX and Gag and thereby mediate  
452 more efficient viral budding. Indeed, co-immunoprecipitation of HIV-1C Gag-PYKE was more  
453 efficient compared to the Gag-PYQE variant. As the PYKE motif insertion seems to be the  
454 original insertion within HIV-1C Gag, ubiquitination of its lysine might not be essential since  
455 other variants of the PYKE motif, i.e., PYQE and PYRE, are identified among HIV-1C strains  
456 along with the evolution of another lysine (K) residues in the late domain. Because we only have  
457 few clinical strains with a PY<sub>x</sub>E insertion, we could not identify differences in viral growth  
458 between HIV-1C Gag-PYKE and other PY<sub>x</sub>E variants. Nonetheless, whereas the other three  
459 residues seem to be required for the binding of ALIX to Gag, the lysine residue might provide  
460 increased stability for this interaction.

461 Although the ALIX-mediated viral budding mechanism appeared to be lost in HIV-1C, it is  
462 surprising to observe that HIV-1C PY<sub>x</sub>E strains were prevalent among HIV-1C infected  
463 individuals. This suggests that the interaction of Gag with ALIX is of biological importance for  
464 the virus. In our limited cohort of HIV-1C infected patients, PY<sub>x</sub>E insertion was always co-  
465 present with the PTAP motif. This suggests that the PY<sub>x</sub>E motif is not redundant from the PTAP  
466 motif-mediated viral budding process through TSG101 nor a compensatory mechanism for loss  
467 of the PTAP-motif and HIV-1 requires both motifs for efficient viral replication. Importantly,



468 viruses with HIV-1C Gag PYKE or PYQE insertion showed enhanced viral growth compared to  
469 viruses with HIV-1C wild type Gag (Fig.5). This finding is in line with a recent report that  
470 showed that a PYRE insertion within Gag enhances HIV-1C viral growth (19).

471 Decreased sensitivity towards PI LPV or NRTI TAF was found in several HIV-1C strains with a  
472 PTAP duplication or PYxE insertion. For the PTAP duplication, it has previously been reported  
473 that it could enhance HIV-1 growth in the presence of PIs lopinavir and ritonavir (26). For the  
474 PYxE insertion, our earlier studies have shown that the PYxE insertion is more frequent in HIV-  
475 1C therapy-failure patients (15, 16). Nonetheless, since our clinical HIV-1C PYxE strains did not  
476 have any known drug resistance mutations, it seems likely that the correlation of these viruses  
477 with advanced viral growth and reduced sensitivity towards the PI LPV and TAF could increase  
478 the risk for therapy failure in HIV-1C PYxE-infected patients. Mechanistic studies show that at  
479 the time of reverse transcription of HIV-1C from the RNA template, the RT favors pausing at the  
480 nucleotides in HIV-1C K65 position (AAG) and this correlates with increased probability for the  
481 development of TDF/TAF mutation K65R (38, 39). However, no studies have shown any co-  
482 relation with Gag-mutation on the susceptibility of TAF. We are presently performing research to  
483 understand the role of Gag mutations on sensitivity for TAF as both tenofovir (TDF) and TAF are  
484 used globally.

485 In conclusion, our study showed that PYxE insertion in HIV-1C of patients originating from  
486 Ethiopia and Eritrea restored the interaction of Gag with ALIX, which is mediated in an  
487 ubiquitin-dependent or -independent way. Importantly, the insertion was positively correlated  
488 with the replication fitness that could affect the sensitivity against LPV in the absence of any PI  
489 drug resistance mutation. Based on the present study, our earlier clinical studies (15-17) and the  
490 study by Chaturbhuj et al. (19), we posit that a PYxE insertion in HIV-1 subtype C strains  
491 provides a replication advantage that can affect the susceptibility of the virus to certain  
492 antiretroviral drugs. As the PYxE insertion evolved within treatment failure patients infected with  
493 HIV-1C from both India and South Africa, HIV-1C<sub>PYxEi</sub> also provides a replication advantage  
494 following treatment failure and following evolution of drug resistance mutations that may cost  
495 replication fitness. Most importantly, reduced sensitivity against TAF in the absence of any TAF-  
496 mutation needs further studies to analyze any role of Gag-mutations in reducing susceptibility  
497 towards TAF. Altogether, it will be important to follow up on whether HIV-1C<sub>PYxEi</sub> strains are  
498 emerging following the failure of antiretroviral therapy with LPV and TAF based regimens due

499 to increased replication fitness. This information could provide important insights into the clinical  
500 significance of the PYxE insertion within HIV-1C Gag.

#### 501 **Acknowledgments**

502 The study is funded by grants from the Swedish Research Council (2017-01330, UN; 2016-  
503 01675, AS), Karolinska Institutet Doctoral Student Funding (KID2015-154, UN) and the  
504 Stockholm County Council (ALF 20160074, AS). We thank S.G. Aralaguppe, W. Zhang and S.  
505 Svensson Akusjärvi for technical assistance. The microscopic part of the study was performed at  
506 the Live Cell Imaging facility, Karolinska Institutet, Sweden, supported by grants from the Knut  
507 and Alice Wallenberg Foundation, the Swedish Research Council, the Centre for Innovative  
508 Medicine and the Jonasson center at the Royal Institute of Technology, Sweden. The following  
509 reagents were obtained through the AIDS Reagent Program, Division of AIDS, NIAID, NIH:  
510 TZM-bl cells (Cat#8129) from Dr. John C. Kappes, and Dr. Xiaoyun Wu, MT-4 cells from Dr.  
511 Douglas Richman, and HIV-1 NL4-3 Infectious Molecular Clone (pNL4-3) from Dr. Malcolm  
512 Martin (Cat#114).

513

#### 514 **References**

- 515 1. **Siddik AB, Haas A, Rahman MS, Aralaguppe SG, Amogne W, Bader J, Klimkait T, Neogi U.** 2018.  
516 Phenotypic co-receptor tropism and Maraviroc sensitivity in HIV-1 subtype C from East Africa. *Sci*  
517 *Rep* **8**:2363.
- 518 2. **Neogi U, Haggblom A, Santacatterina M, Bratt G, Gisslen M, Albert J, Sonnerborg A.** 2014.  
519 Temporal trends in the Swedish HIV-1 epidemic: increase in non-B subtypes and recombinant  
520 forms over three decades. *PLoS One* **9**:e99390.
- 521 3. **Sundquist WI, Krausslich HG.** 2012. HIV-1 assembly, budding, and maturation. *Cold Spring Harb*  
522 *Perspect Med* **2**:a006924.
- 523 4. **Bieniasz PD.** 2006. Late budding domains and host proteins in enveloped virus release. *Virology*  
524 **344**:55-63.
- 525 5. **Demirov DG, Freed EO.** 2004. Retrovirus budding. *Virus Res* **106**:87-102.
- 526 6. **Votteler J, Sundquist WI.** 2013. Virus budding and the ESCRT pathway. *Cell Host Microbe*  
527 **14**:232-241.
- 528 7. **Martin-Serrano J, Neil SJ.** 2011. Host factors involved in retroviral budding and release. *Nat Rev*  
529 *Microbiol* **9**:519-531.
- 530 8. **Scourfield EJ, Martin-Serrano J.** 2017. Growing functions of the ESCRT machinery in cell biology  
531 and viral replication. *Biochem Soc Trans* **45**:613-634.
- 532 9. **Flys T, Marlowe N, Hackett J, Parkin N, Schumaker M, Holzmayer V, Hay P, Eshleman SH.** 2005.  
533 Analysis of PTAP duplications in the gag p6 region of subtype C HIV type 1. *AIDS Res Hum*  
534 *Retroviruses* **21**:739-741.

- 535 10. **Sharma S, Aralaguppe SG, Abrahams MR, Williamson C, Gray C, Balakrishnan P, Saravanan S,**  
536 **Murugavel KG, Solomon S, Ranga U.** 2017. The PTAP sequence duplication in HIV-1 subtype C  
537 Gag p6 in drug-naive subjects of India and South Africa. *BMC Infect Dis* **17**:95.
- 538 11. **Garrus JE, von Schwedler UK, Pornillos OW, Morham SG, Zavitz KH, Wang HE, Wettstein DA,**  
539 **Stray KM, Cote M, Rich RL, Myszka DG, Sundquist WI.** 2001. Tsg101 and the vacuolar protein  
540 sorting pathway are essential for HIV-1 budding. *Cell* **107**:55-65.
- 541 12. **Fisher RD, Chung HY, Zhai Q, Robinson H, Sundquist WI, Hill CP.** 2007. Structural and  
542 biochemical studies of ALIX/AIP1 and its role in retrovirus budding. *Cell* **128**:841-852.
- 543 13. **Patil A, Bhattacharya J.** 2012. Natural deletion of L35Y36 in p6 gag eliminate LYPXnL/ALIX  
544 auxiliary virus release pathway in HIV-1 subtype C. *Virus Res* **170**:154-158.
- 545 14. **Zhai Q, Landesman MB, Robinson H, Sundquist WI, Hill CP.** 2011. Identification and structural  
546 characterization of the ALIX-binding late domains of simian immunodeficiency virus SIVmac239  
547 and SIVagmTan-1. *J Virol* **85**:632-637.
- 548 15. **Neogi U, Rao SD, Bontell I, Verheyen J, Rao VR, Gore SC, Soni N, Shet A, Schulter E, Ekstrand**  
549 **ML, Wondwossen A, Kaiser R, Madhusudhan MS, Prasad VR, Sonnerborg A.** 2014. Novel tetra-  
550 peptide insertion in Gag-p6 ALIX-binding motif in HIV-1 subtype C associated with protease  
551 inhibitor failure in Indian patients. *Aids* **28**:2319-2322.
- 552 16. **Neogi U, Engelbrecht S, Claassen M, Jacobs GB, van Zyl G, Preiser W, Sonnerborg A.** 2016.  
553 Mutational Heterogeneity in p6 Gag Late Assembly (L) Domains in HIV-1 Subtype C Viruses from  
554 South Africa. *AIDS Res Hum Retroviruses* **32**:80-84.
- 555 17. **Aralaguppe SG, Winner D, Singh K, Sarafianos SG, Quinones-Mateu ME, Sonnerborg A, Neogi**  
556 **U.** 2017. Increased replication capacity following evolution of PYxE insertion in Gag-p6 is  
557 associated with enhanced virulence in HIV-1 subtype C from East Africa. *J Med Virol* **89**:106-111.
- 558 18. **Kiguoya MW, Mann JK, Chopera D, Gounder K, Lee GQ, Hunt PW, Martin JN, Ball TB, Kimani J,**  
559 **Brumme ZL, Brockman MA, Ndung'u T.** 2017. Subtype-Specific Differences in Gag-Protease-  
560 Driven Replication Capacity Are Consistent with Intersubtype Differences in HIV-1 Disease  
561 Progression. *J Virol* **91**.
- 562 19. **Chaturbhuj D, Patil A, Gangakhedkar R.** 2018. PYRE insertion within HIV-1 subtype C p6-Gag  
563 functions as an ALIX-dependent late domain. *Sci Rep* **8**:8917.
- 564 20. **Neogi U, Singh K, Aralaguppe SG, Rogers LC, Njenda DT, Sarafianos SG, Hejdeman B,**  
565 **Sonnerborg A.** 2018. Ex-vivo antiretroviral potency of newer integrase strand transfer inhibitors  
566 cabotegravir and bictegravir in HIV type 1 non-B subtypes. *Aids* **32**:469-476.
- 567 21. **Zhai Q, Fisher RD, Chung HY, Myszka DG, Sundquist WI, Hill CP.** 2008. Structural and functional  
568 studies of ALIX interactions with YPX(n)L late domains of HIV-1 and EIAV. *Nat Struct Mol Biol*  
569 **15**:43-49.
- 570 22. **Sundquist WI, Schubert HL, Kelly BN, Hill GC, Holton JM, Hill CP.** 2004. Ubiquitin recognition by  
571 the human TSG101 protein. *Mol Cell* **13**:783-789.
- 572 23. **Schindelin J, Arganda-Carreras I, Frise E, Kaynig V, Longair M, Pietzsch T, Preibisch S, Rueden C,**  
573 **Saalfeld S, Schmid B, Tinevez JY, White DJ, Hartenstein V, Eliceiri K, Tomancak P, Cardona A.**  
574 2012. Fiji: an open-source platform for biological-image analysis. *Nat Methods* **9**:676-682.
- 575 24. **Sette P, Nagashima K, Piper RC, Bouamr F.** 2013. Ubiquitin conjugation to Gag is essential for  
576 ESCRT-mediated HIV-1 budding. *Retrovirology* **10**:79.
- 577 25. **Sharma S, Arunachalam PS, Menon M, Ragupathy V, Satya RV, Jebaraj J, Ganeshappa**  
578 **Aralaguppe S, Rao C, Pal S, Saravanan S, Murugavel KG, Balakrishnan P, Solomon S, Hewlett I,**  
579 **Ranga U.** 2018. PTAP motif duplication in the p6 Gag protein confers a replication advantage on  
580 HIV-1 subtype C. *J Biol Chem* doi:10.1074/jbc.M117.815829.

- 581 26. **Martins AN, Waheed AA, Ablan SD, Huang W, Newton A, Petropoulos CJ, Brindeiro RD, Freed**  
582 **EO.** 2016. Elucidation of the Molecular Mechanism Driving Duplication of the HIV-1 PTAP Late  
583 Domain. *J Virol* **90**:768-779.
- 584 27. **Wright JK, Brumme ZL, Carlson JM, Heckerman D, Kadie CM, Brumme CJ, Wang B, Losina E,**  
585 **Miura T, Chonco F, van der Stok M, Mncube Z, Bishop K, Goulder PJ, Walker BD, Brockman MA,**  
586 **Ndung'u T.** 2010. Gag-protease-mediated replication capacity in HIV-1 subtype C chronic  
587 infection: associations with HLA type and clinical parameters. *J Virol* **84**:10820-10831.
- 588 28. **Singh K, Flores JA, Kirby KA, Neogi U, Sonnerborg A, Hachiya A, Das K, Arnold E, McArthur C,**  
589 **Parniak M, Sarafianos SG.** 2014. Drug resistance in non-B subtype HIV-1: impact of HIV-1 reverse  
590 transcriptase inhibitors. *Viruses* **6**:3535-3562.
- 591 29. **Bello NF, Wu F, Sette P, Dussupt V, Hirsch VM, Bouamr F.** 2011. Distal leucines are key  
592 functional determinants of Alix-binding simian immunodeficiency virus SIV(smE543) and  
593 SIV(mac239) type 3 L domains. *J Virol* **85**:11532-11537.
- 594 30. **Amogne W, Bontell I, Grossmann S, Aderaye G, Lindquist L, Sonnerborg A, Neogi U.** 2016.  
595 Phylogenetic Analysis of Ethiopian HIV-1 Subtype C Near Full-Length Genomes Reveals High  
596 Intrasubtype Diversity and a Strong Geographical Cluster. *AIDS Res Hum Retroviruses* **32**:471-  
597 474.
- 598 31. **Tully DC, Wood C.** 2010. Chronology and evolution of the HIV-1 subtype C epidemic in Ethiopia.  
599 *Aids* **24**:1577-1582.
- 600 32. **Demirov DG, Orenstein JM, Freed EO.** 2002. The late domain of human immunodeficiency virus  
601 type 1 p6 promotes virus release in a cell type-dependent manner. *J Virol* **76**:105-117.
- 602 33. **Huang M, Orenstein JM, Martin MA, Freed EO.** 1995. p6Gag is required for particle production  
603 from full-length human immunodeficiency virus type 1 molecular clones expressing protease. *J*  
604 *Virol* **69**:6810-6818.
- 605 34. **Strack B, Calistri A, Craig S, Popova E, Gottlinger HG.** 2003. AIP1/ALIX is a binding partner for  
606 HIV-1 p6 and EIAV p9 functioning in virus budding. *Cell* **114**:689-699.
- 607 35. **Dussupt V, Javid MP, Abou-Jaoude G, Jadwin JA, de La Cruz J, Nagashima K, Bouamr F.** 2009.  
608 The nucleocapsid region of HIV-1 Gag cooperates with the PTAP and LYPXnL late domains to  
609 recruit the cellular machinery necessary for viral budding. *PLoS Pathog* **5**:e1000339.
- 610 36. **Gottwein E, Jager S, Habermann A, Krausslich HG.** 2006. Cumulative mutations of ubiquitin  
611 acceptor sites in human immunodeficiency virus type 1 gag cause a late budding defect. *J Virol*  
612 **80**:6267-6275.
- 613 37. **Zhadina M, McClure MO, Johnson MC, Bieniasz PD.** 2007. Ubiquitin-dependent virus particle  
614 budding without viral protein ubiquitination. *Proc Natl Acad Sci U S A* **104**:20031-20036.
- 615 38. **Coutsinos D, Invernizzi CF, Moisi D, Oliveira M, Martinez-Cajas JL, Brenner BG, Wainberg MA.**  
616 2011. A template-dependent dislocation mechanism potentiates K65R reverse transcriptase  
617 mutation development in subtype C variants of HIV-1. *PLoS One* **6**:e20208.
- 618 39. **Coutsinos D, Invernizzi CF, Xu H, Moisi D, Oliveira M, Brenner BG, Wainberg MA.** 2009.  
619 Template usage is responsible for the preferential acquisition of the K65R reverse transcriptase  
620 mutation in subtype C variants of human immunodeficiency virus type 1. *J Virol* **83**:2029-2033.
- 621
- 622

623 **Tables**

624 Table 1. List of amino acids that are involved in the interaction between Gag-P6, ALIX and  
 625 ubiquitin (Ub).

626

Interacting atoms	Residue 1	Residue 2	Distance (Å)	Interaction type
<b>OE1 – NH1</b>	E482 (LD)	R386 (ALIX)	2.96	Charge-charge
<b>OE2 – NH2</b>	E482 (LD)	R386 (ALIX)	2.83	Charge-charge
<b>OE1 – NZ</b>	E387 (ALIX)	K63 (Ub)	3.05	Charge-charge
<b>OE2 – NZ</b>	E387 (ALIX)	K63 (Ub)	2.97	Charge-charge
<b>OE2 – NZ</b>	E64 (Ub)	K485 (LD)	2.93	Charge-charge
<b>OE2 – NZ</b>	E486 (LD)	K501 (ALIX)	2.95	Charge-charge
<b>OE1 – NZ</b>	E16 (Ub)	K501 (ALIX)	3.12	Charge-charge
<b>OH – OD1</b>	Y484 (LD)	D506 (ALIX)	2.72	Hydrogen Bond

627 E = glutamic acid, R = arginine, Y = tyrosine, D = aspartic acid, K = lysine

628

629 **Figure legends**

630 **Figure 1. Consensus sequences and distribution of HIV-1 gag.** (a) Aligned consensus  
 631 sequences of a gag from HIV-1 type B wild-type (top), HIV-1 type C wild-type (middle), and  
 632 HIV-1 type C with tetrapeptide insertion (bottom) from the Los Alamos database. Sequence  
 633 logos with one-letter coded amino acid were generated using WebLogo 3. (b-d) Distribution of  
 634 HIV-1 type C with gag<sub>wt</sub>, gag<sub>PYKE</sub>, and gag<sub>PYQE</sub> in patient cohorts from Sweden (b), Germany (c)  
 635 and Ethiopia (d).

636 **Figure 2. Cellular localization of Gag variants and ALIX.** Confocal images of HEK293T cells  
 637 co-transfected with the GFP-tagged ALIX and mCherry-tagged HIV-1C Gag variants (wt,  
 638 PYKEi, & PYQEi) expression plasmids. Nuclei are visualized in blue, ALIX in green, and Gag in  
 639 red. Bars, 20 μm.

640 **Figure 3. HIV-1C Gag with PYxE insertion has increased binding with ALIX.** (a-d) Protein-  
 641 peptide interaction using Microscale thermophoresis. The peptide sequences are given in the  
 642 individual graphs. (e) The equilibrium dissociation constant (K<sub>d</sub>) of the individual interactions.  
 643 The smaller the K<sub>d</sub> value, the greater the binding affinity of the ligand for its target. (f) HEK293T  
 644 cells were co-transfected with GFP-tagged ALIX and Gag variants from HIV-1 type B or C. At

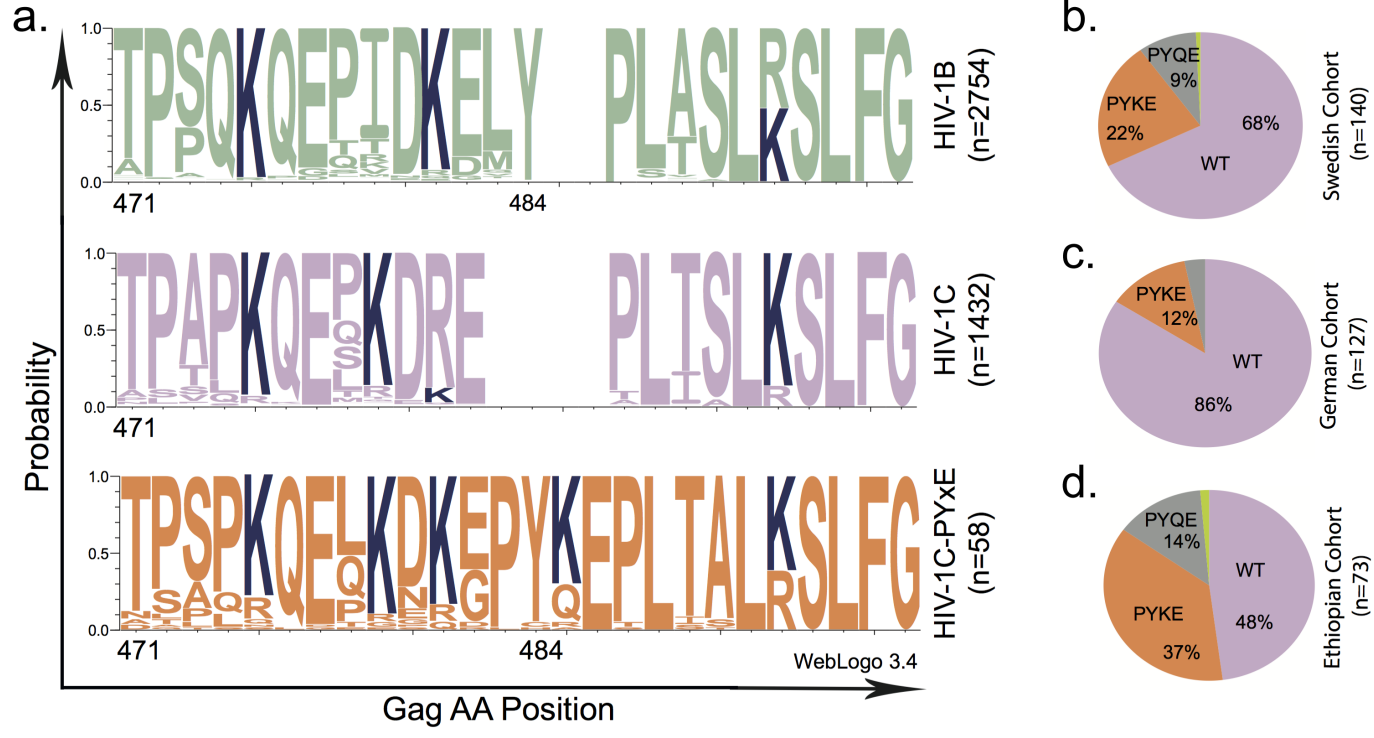
645 24 hours post-transfection, cells were lysed and subjected to GFP-pull down. Input and pull-down  
646 samples were subjected to immunoblotting antibodies against GFP (ALIX), p55 (Gag), and  $\beta$ -  
647 actin. Data depicted are representative of at least two independent experiments.

648 **Figure 4. *In silico* binding prediction between PYKE inserted within HIV-1 type C Gag,**  
649 **ALIX, and ubiquitin. (a)** Likelihood of ubiquitin binding to lysine residues in the vicinity of or  
650 within the PYKE motif.  $K_{ins}$  represents the lysine residue within the PYKE motif. **(b)** All proteins  
651 are presented as ribbon-like structures. The red ribbon represents Gag and its PYKE insertion, the  
652 blue ribbon ALIX and its Gag-binding sites, and the green ribbon ubiquitin. Amino acids  
653 involved in Gag: ALIX binding is shown in one-letter format. Interactions between amino acids  
654 are shown with black dotted lines. *In silico* docking was performed using Schrödinger software.  
655 **(c)** Confocal images of HEK293T cells transfected with the GFP-tagged ALIX and mCherry-  
656 tagged HIV-1C Gag PYQEi and HA-tagged ubiquitin expression plasmids. Nuclei are visualized  
657 in blue, ALIX in green, Gag in red, and ubiquitin in magenta. Bar, 20  $\mu$ m.

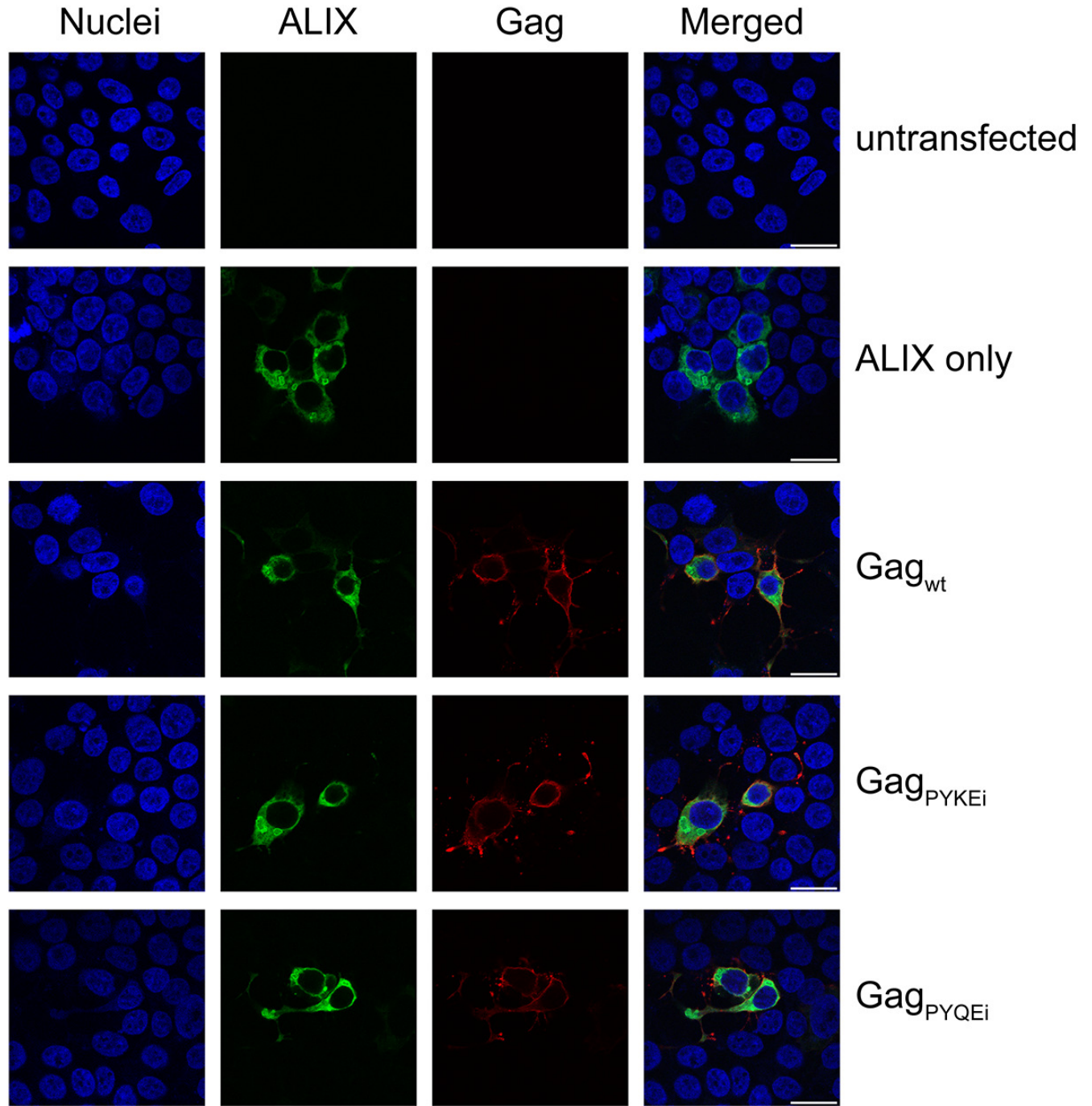
658 **Figure 5. PYxE insertion increases viral growth and drug sensitivity towards protease**  
659 **inhibitor drug lopinavir (a)** Gag-pol sequences were amplified from HIV-1 type C patient  
660 isolates and cloned into HIV-1 molecular clone pNL4-3. Recombinant viruses were propagated in  
661 HEK293T cells and MOIs were determined in TZM-bl reporter cells. Viral growth assay was  
662 performed in MT-4 cells **(b)** or purified primary CD4<sup>+</sup> T cells **(c)**. Cells were infected with the  
663 various recombinant viruses at an MOI of 0.05 and supernatants were harvested on day 0, 3, 5,  
664 and 7. Viral load in supernatants were measured by HIV-1 p24 analysis on the HIV COBAS 8000  
665 platform. Data represent the mean  $\pm$  SD of triplicates. Clinical data regarding viral load at  
666 initiation of therapy **(d)**, CD4<sup>+</sup> T cell count at initiation of therapy **(e)**, and nadir CD4<sup>+</sup> T cell  
667 count **(f)** was collected from the Swedish HIV-1C cohort and patients were grouped as HIV-  
668 1C<sub>PYxEi</sub> (n=45) or HIV-1C<sub>WT</sub> infected individuals (n=95).

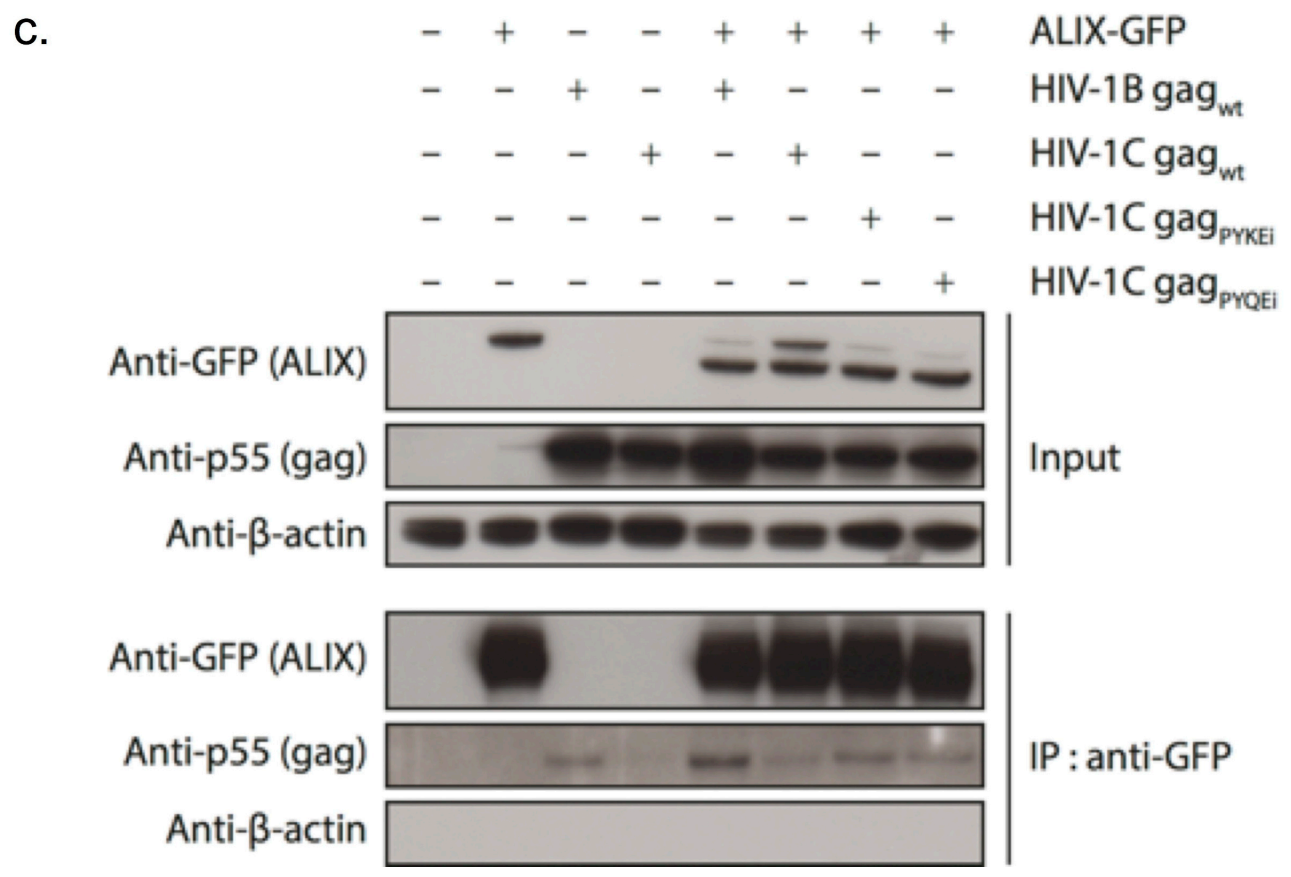
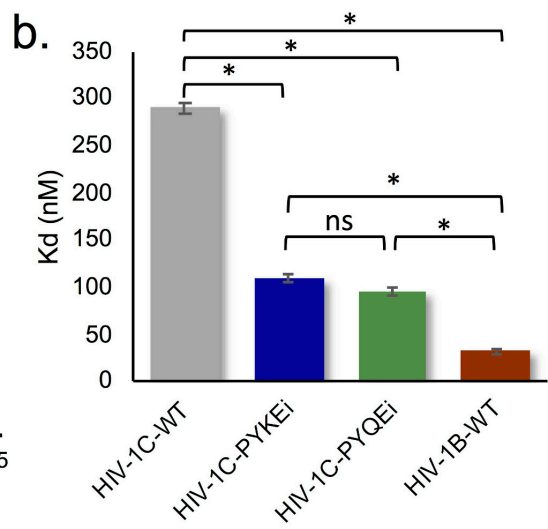
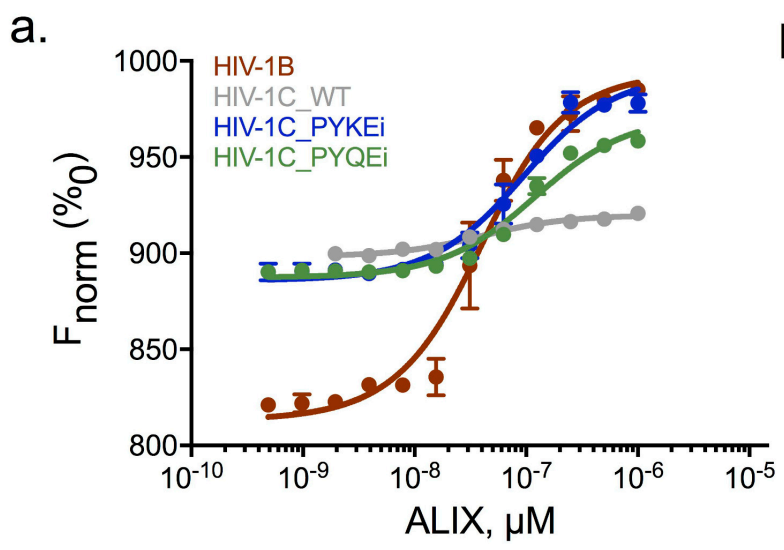
669 **Figure 6. PYxE insertion increases drug sensitivity towards protease inhibitor drug**  
670 **lopinavir.** TZM-bl reporter cells were infected with the individual recombinant HIV viruses at an  
671 MOI of 0.05 and cultured in the presence of individual anti-retroviral drugs at different dilutions.  
672 EC<sub>50</sub> values for each virus with each drug were determined and EC<sub>50</sub> fold changes (FC) were  
673 calculated compared to pNL4-3 reference virus. PI, protease inhibitor; NRTI, Nucleoside Reverse  
674 Transcriptase Inhibitor; NNRTI, Non-Nucleoside Reverse Transcriptase Inhibitor; INSTI,

675 Integrase Strand Transfer Inhibitor. ATV, Atazanavir sulfate; DRV, darunavir ethanoate; LPV,  
676 lopinavir; AZT, azidothymidine; TAF, tenofovir alafenamide; EFV, efavirenz; RPV, rilpivirine;  
677 ETR, etravirine; RAL, raltegravir; EVG, elvitegravir; DTG, dolutegravir; CAB, cabotegravir.  
678 The FC data presented in the heat map was the mean of three individual experiments.

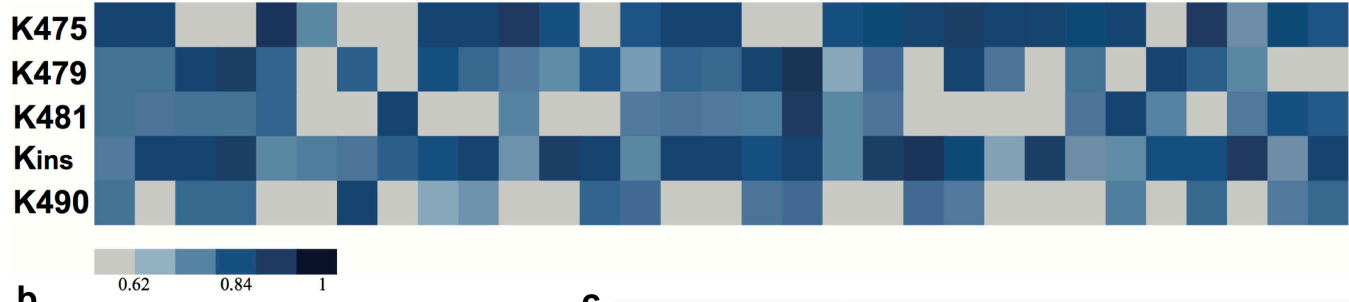




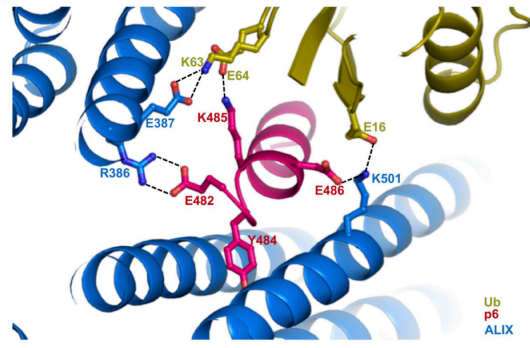




a.



b.



c.

